27th EPS Conference on Contr. Fusion and Plasma Phys. Budapest, 12-16 June 2000 ECA Vol. **24B** *(2000) 676 -679*

The $1/\nu$ transport regime for neoclassically optimized stellarator systems*

Viktor V. Nemov[1], Sergei V. Kasilov[1], **Winfried Kernbichler**[2], Martin F. Heyn[2], Joseph Talmadge[3]

[1]*Institute of Plasma Physics, National Science Center "Kharkov Institute of Physics and Technology", Ul. Akademicheskaya 1, 310108 Kharkov, Ukraine*
[2]*Institut für Theoretische Physik, Technische Universität Graz, Petersgasse 16, A–8010 Graz, Austria*
[3]*University of Wisconsin-Madison, USA*

Introduction

Minimization of neoclassical transport in the so called $1/\nu$ regime is one of the key issues in stellarator optimization. At present, a number of stellarator devices with such an optimization are under elaboration and it is of interest to compare the degree of optimization which can be achieved. For this purpose, fast and convenient methods are desirable. Here, the $1/\nu$ transport is analyzed for two new stellarator devices W7-X [1] and HSX [2] with the use of the new computational method formulated in [3]. Within this method, the neoclassical transport coefficients are calculated by taking into account all classes of trapped particles. Therefore, the results are valid for arbitrary magnetic field geometries with intact flux surfaces.

Basic equations and parameters

As shown in [3], the particle flux density, F_n, averaged over a magnetic surface, can be presented in the form,

$$F_n = -\frac{\sqrt{8}}{9\pi^{3/2}}\frac{v_T^2\rho_L^2}{\nu R^2}\epsilon_{\rm eff}^{3/2}\int\limits_0^\infty \frac{{\rm d}z\, e^{-z}z^{5/2}}{A(z)}\frac{n}{f_M}\frac{\partial f_M}{\partial r}, \tag{1}$$

$$\epsilon_{\rm eff}^{3/2} = \frac{\pi R^2}{8\sqrt{2}}\lim_{L_s\to\infty}\left(\int\limits_0^{L_s}\frac{ds}{B}\right)\left(\int\limits_0^{L_s}\frac{ds}{B}|\nabla\psi|\right)^{-2}\int\limits_{B_{min}^{(abs)}/B_0}^{B_{max}^{(abs)}/B_0}{\rm d}b'\sum_{j=1}^{j_{max}}\frac{\hat{H}_j^2}{\hat{I}_j}\,, \tag{2}$$

$$\hat{H}_j = \frac{1}{b'}\int\limits_{s_j^{(min)}}^{s_j^{(max)}}\frac{{\rm d}s}{B}\sqrt{b'-\frac{B}{B_0}}\left(4\frac{B_0}{B}-\frac{1}{b'}\right)|\nabla\psi|k_G, \quad \hat{I}_j = \int\limits_{s_j^{(min)}}^{s_j^{(max)}}\frac{{\rm d}s}{B}\sqrt{1-\frac{B}{B_0b'}}\,. \tag{3}$$

Here, $f_M = f_M(\psi, w)$ is the Maxwellian distribution, $n(\psi)$ is the particle density, ψ is the magnetic surface label, $w = mv^2/2 + e\Phi$ is the particle energy, $v_T = \sqrt{2T/m}$ is the thermal velocity, $\rho_L = mcv_T/(eB_0)$ is the mean Larmor radius, $A(z)$ is a quantity related to the collision operator, R is the major radius of the torus, $z = mv^2/(2T)$ is the normalized energy, $\partial f_M/\partial r$ is the average normal derivative, and $k_G = (\mathbf{h}\times(\mathbf{h}\cdot\nabla)\mathbf{h})\cdot\nabla\psi/|\nabla\psi|$ is the geodesic curvature of a magnetic field line ($\mathbf{h} = \mathbf{B}/B$). The characteristic features of the specific magnetic field geometry manifest themselves through the factor $\epsilon_{\rm eff}^{3/2}$, where $\epsilon_{\rm eff}$ is the effective ripple modulation amplitude. This factor takes into account the contributions from

*This work has been carried out within the Association EURATOM-ÖAW.

particles trapped within single or multiple magnetic wells to the $1/\nu$ transport. The quantity $\epsilon_{\rm eff}$ is computed by integration over the magnetic field line length, s, over a sufficiently large interval $0 \div L_s$ as well as over the perpendicular adiabatic invariant of trapped particles, i.e., the variable b'. $B_{min}^{(abs)}$ and $B_{max}^{(abs)}$ are the minimum and maximum values of B within the interval of $0 \div L_s$. The quantities $s_j^{(min)}$ and $s_j^{(max)}$ in the sum over j in (2) correspond to the reflection points of trapped particles. The result (1) differs from the corresponding formula for the classical stellarator model [4] by the replacement of the helical modulation amplitude along the magnetic field line $\epsilon_{\rm h}$ with the quantity $\epsilon_{\rm eff}$. Therefore, for any magnetic configuration, the $1/\nu$ transport coefficients can be obtained from the appropriate coefficients for the classical stellarator with the replacement of $\epsilon_{\rm h}$ by $\epsilon_{\rm eff}$.

Formulas (1)-(2) are applied to study the $1/\nu$ transport in the W7-X ($n_p = 5$) and in the HSX ($n_p = 4$) magnetic configurations [1,2] (n_p is the number of magnetic field periods in the device) for the case of negligible plasma pressure, $\beta = 0$. In this case, only the magnetic field produced by the coil currents is taken into account. The calculations are done in real space coordinates. For HSX the magnetic field (and its spatial derivatives) are computed from the Biot-Savart law. The W7-X magnetic field is presented as a superposition of a finite number (465) of toroidal harmonic functions containing the associated Legendre functions. To find the decomposition coefficients we used the boundary surface equation given in [5]. Together with HSX, also the configuration HSX-M with additional mirror coils is considered and compared to the other results.

Figs. 1 and 2 show cross-sections of magnetic surfaces used for the $\epsilon_{\rm eff}^{3/2}$ computations of HSX and W7-X (standard version [5]). Not shown are the magnetic surfaces for HSX-M which have approximately the same shape as those for HSX. However, due to the strong stochasticity of the magnetic field lines near the boundary of the HSX-M configuration (and the magnetic islands there), the good confinement region for this configuration is somewhat smaller than that for the HSX configuration. Fig. 3 shows the rotational transform for all considered configurations.

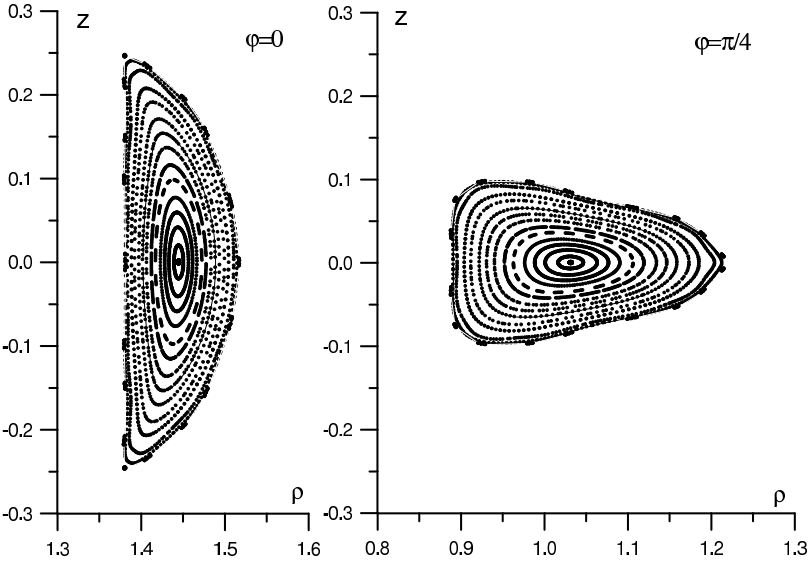

Fig. 1. Magnetic surfaces for the HSX configuration in the ρ, φ, z coordinate system. For the starting point at $\rho = 1.521$ (with $\varphi = 0$ and $z = 0$) the field line is lost after 66 magnetic field periods; the starting point at $\rho = 1.517$ corresponds to an island magnetic surface with ι =10/9.

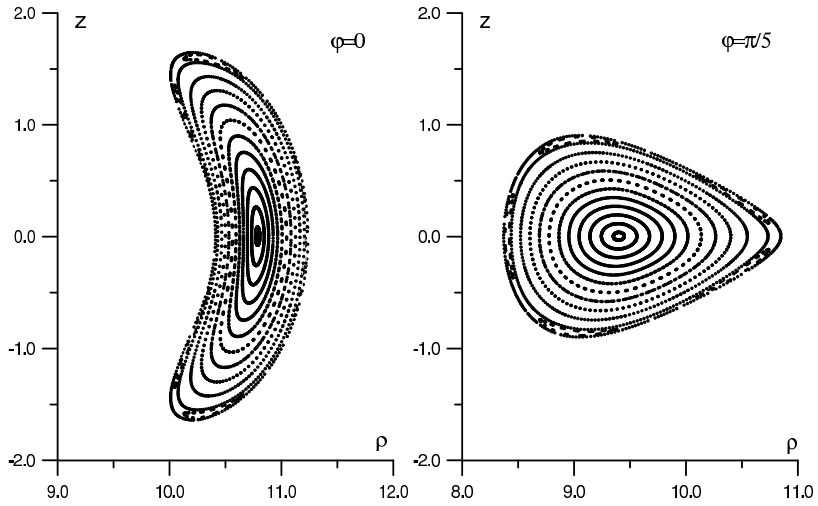

Fig. 2. Magnetic surfaces for the W7-X configuration (standard version). The outer surface coincides with the boundary surface [5] used to obtain the magnetic field decomposition. An island region corresponding to ι=1 is seen near the boundary.

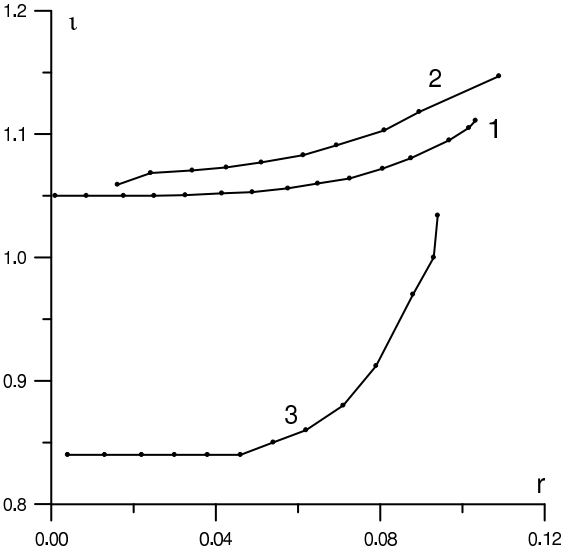

Fig. 3. Rotational transform vs. mean magnetic surface radius (in units of the big torus radius) for the HSX (1), HSX-M (2) and W7-X (3) configurations.

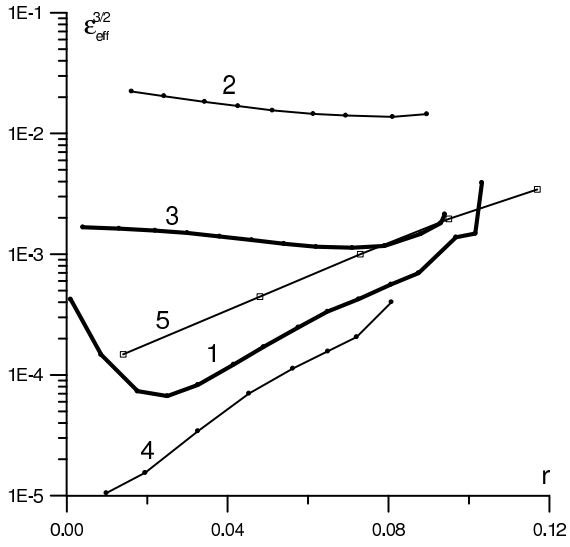

Fig. 4. Parameter $\epsilon_{\rm eff}^{3/2}$ vs. mean magnetic surface radius for the HSX (1), HSX-M (2) and W7-X (3) configurations. For comparison, also the results for the QHS (4) and the drift-optimized CHS (5) configurations are shown.

Results

Computational results for $\epsilon_{\rm eff}^{3/2}$ are presented in Fig. 4 as functions of the mean magnetic surface radius r expressed in units of the big torus radius or, for HSX, in units of the radius were the magnetic axis is located. For comparison, also the results of previous computations for the quasi-helically symmetric configuration (QHS) and the drift-optimized version of CHS (see [3] and [6]) are shown.

It follows from Fig. 4 that the HSX-M configuration does not possess good symmetry properties and therefore $\epsilon_{\rm eff}^{3/2}$ is close to the value of the standard stellarator. In contrast to this configuration, the results for HSX demonstrate the excellent quasi-symmetry properties of this device. For almost all values of r, $\epsilon_{\rm eff}^{3/2}$ is two orders of magnitude less than that for the standard stellarator. Only near the boundary, $\epsilon_{\rm eff}^{3/2}$ is somewhat higher and reaches $\epsilon_{\rm eff}^{3/2} = 1.48 \times 10^{-3}$ for r=0.1016 (ρ=1.515). This value is approximately two times smaller than that for the

W7-X configuration. With growing r (r=0.1032, ρ =1.517), $\epsilon_{\rm eff}^{3/2}$ shows a sharp increase up to $\epsilon_{\rm eff}^{3/2} = 3.9 \times 10^{-3}$ for the island magnetic surface with ι=10/9. The $\epsilon_{\rm eff}^{3/2}$ value also increases towards the magnetic axis. This can be explained by the discrete character of the HSX coil distribution.

For the standard version of W7-X, $\epsilon_{\rm eff}^{3/2}$ varies from 1.13×10^{-3} to 2.14×10^{-3}. This is one order of magnitude less than for the standard stellarator being in agreement with [1]. Note that there is no essential increase in $\epsilon_{\rm eff}^{3/2}$ for the island surface (ι=1) shown in Fig. 2. The $\epsilon_{\rm eff}^{3/2}$ values computed for the low-ι and the high-ι versions of W7-X (see [5]) turn out to be only slightly larger than the values for the standard version (up to 2.7×10^{-3} and 3.3×10^{-3}, respectively). It follows from Fig. 4 that the drift-optimized version of CHS shows rather good properties with respect to 1/ν transport (see [6]). For this configuration, $\epsilon_{\rm eff}^{3/2}$ reaches the value of 1.49×10^{-2} for r=0.171. At the edge, this is comparable with $\epsilon_{\rm eff}^{3/2}$ for the standard stellarator. However, within the r limits corresponding to the W7-X device, results for the drift-optimized version of CHS do not exceed those for W7-X.

The lowest value of $\epsilon_{\rm eff}^{3/2}$ is achieved in the QHS configuration [3] which is a real space realization of the original quasi-helically symmetric stellarator [7].

Summary

Employing a newly developed technique [3] which is based on an integration along magnetic field lines, the 1/ν transport coefficients are studied numerically for various optmized stellarator configurations. The method takes into account all classes of trapped particles and has no limitation with respect to the number of magnetic wells along field lines. Calculations are done for various versions of the W7-X configuration [1,5] and for the quasi-helically symmetric stellarator HSX [2]. These results are also compared to results from previous computations for the quasi-helically symmetric configuration (QHS) and the drift-optimized version of CHS (see [3] and [6]). The results show that the level of 1/ν transport for various versions of W7-X [5] is by one order of magnitude less than that for the standard stellarator. For HSX this level is even lower. In a significant range of the mean magnetic surface radius, the 1/ν transport reaches values which are two orders of magnitude less than those for the standard stellarator. However, also this level is somewhat higher than the corresponding level for the QHS configuration.

References

[1] G. Grieger *et al., Phys. Fluids B* **4**, 2081 (1992).

[2] A. F. Almagri, D. T. Anderson, S. F. B. Anderson, P. H. Probert, J. L. Shohet, J. N. Talmadge, *IEEE Transactions on Plasma Science* **27**, 114 (1999)

[3] V. V. Nemov, S. V. Kasilov, W. Kernbichler and M. F. Heyn, *Phys. Plasmas* **6**, 4622 (1999).

[4] A. A. Galeev and R. Z. Sagdeev, *Reviews in Plasma Physics*, edited by M.A. Leontovich (Consultants Bureau, New York, 1979) **No. 7**, 257 , [see also in *Voprosy Teorii Plazmy* (Atomizdat, Moscow, 1973), **No. 7**, p. 205, in Russian].

[5] C. Nührenberg, *Phys. Plasmas* **3**, 2401 (1996)

[6] M. F. Heyn, S. V.Kasilov, W. Kernbichler, K. Matsuoka, V. V.Nemov, S. Okamura, O. S. Pavlichenko and R. O.Pavlichenko, *XII International Conference on Stellarators*, Madison (1999)

[7] J. Nührenberg and R. Zille, *Phys. Lett. A* **129**, 113 (1988)